The Permian-Triassic Boundary in the Carnic Alps of Austria (Gartnerkofel Region)			Editors: W.T. Holser & H.P. Schönlaub	
Abh. Geol. B.-A.	ISSN 0378-0864 ISBN 3-900312-74-5	Band **45**	S. 123–137	Wien, Mai 1991

The Permian-Triassic of the Gartnerkofel-1 Core (Carnic Alps, Austria): Geochemistry of Common and Trace Elements II – INAA and RNAA

By MOSES ATTREP, Jr., CHARLES J. ORTH & LEONARD R. QUINTANA*)

With 11 Text-Figures and 21 Tables

Carinthia
Carnic Alps
Permian/Triassic Boundary
Geochemistry
Common Elements
Trace Elements

Österreichische Karte 1 : 50.000
Blatt 198

Contents

Zusammenfassung

Aus der Forschungsbohrung Gartnerkofel-1 (Naßfeld, Karnische Alpen, Österreich) wurden 98 Proben mittels instrumenteller Neutronenaktivierungsmethodik (INAA) auf ihre Gehalte an 29 Haupt- und Spurenelementen analysiert. Zusätzlich wurde die Konzentration von Iridium (Ir) in 65 ausgewählten Proben mittels radiochemischer Untersuchungsmethoden gemessen und die Gehalte von Ni, Os, Pt und Au in einigen Proben bestimmt.

Im Kern fanden sich bei 185,57 m und bei 224,52 m Teufe zwei Anomalien von Iridium (233 ppt bzw. 165 ppt). Auffallenderweise fällt das tiefere Maximum mit dem größten negativen Wert von $\delta^{13}C$ im gesamten Kern zusammen, der den Top des Tesero Horizontes charakterisiert. An diesem Punkt und knapp darunter kommt es auch zu auffallenden Änderungen im Verhältnis der Seltenen Erde Elemente untereinander wie auch im Verhältnis zwischen den Seltenen Erde Elementen und Uran zu Aluminium (proportional zu Tongehalt). Wir meinen, daß diese signifikanten Änderungen als eine bevorzugte Fällung dieser Elemente im Ozeanwasser zu interpretieren sind und vielleicht auf aufsteigendes P-reiches Tiefenwasser zurückgehen, das eine Blüte kalkigen Planktons bewirkte.

Die obere Ir-Anomalie fällt mit dem zweiten Negativwert von $\delta^{13}C$ zusammen, der in einer Pyrit-reichen Lage liegt (25 % Fe). Wir vermuten daher einen ursächlichen Zusammenhang zwischen der Bildung dieses Pyrits und der Ir-Anreicherung. Wenn wir auch nicht gänzlich eine extraterrestrische Herkunft für das Iridium in der tieferen Anomalie ausschließen wollen, so spricht doch das Fehlen anderer typischer Impaktmerkmale wie z. B. fehlende „chondritische" Verhältnisse zwischen Ir/Co etc., Mikrosphären oder geschockte Mineralkörner und der vergesellschaftete Anstieg des Sulfidgehaltes gegen diese Annahme. Eher fand ein Anreicherungsprozeß statt, verbunden mit reduzierenden Bedingungen, die sich zeitweise an der Wende vom Perm zur Trias am Meeresboden der frühen Tethys einstellten.

Abstract

Instrumental neutron activation methods were used to determine whole-rock abundances for 29 trace and common elements in 98 samples from the Gartnerkofel-1 core. Iridium (Ir) was determined by radiochemical methods on 65 of these samples and Ni, Os, Pt and Au are reported for a few selected samples. Two Ir abundance maxima were observed, one located at a depth of 185.57 m and the other at about 224.5 m. The lower Ir peak coincides with the most negative excursion of $\delta^{13}C$ in the entire

*) Authors' address: MOSES ATTREP, Jr., CHARLES J. ORTH, LEONARD R. QUINTANA, Isotope and Nuclear Chemistry Division, Los Alamos National Laboratory, Los Alamos, New Mexico 87545, USA.

core, located stratigraphically at the top of the Tesero Horizon. A change in interelement rare-earth ratios, and a noticeable increase in rare-earth and uranium when expressed as ratios to aluminum (roughly proportional to clay content) occur stratigraphically at and just below the Tesero Horizon. We suspect these rather striking changes are the result of increased scavenging of these elements from ocean water, perhaps associated with upwelling of water richer in phosphorous and an accompanying bloom of calcareous plankton. The upper Ir peak coincides with the second most negative excursion of $\delta^{13}C$ and with a pyrite bed (25 % Fe). Here we suspect the Ir enrichment is associated with the pyrite formation. Although we can not completely preclude an impact source for the lower Ir anomaly, the absence of other impact signatures (chondrite ratios for Ir/Co etc., microspheres and shocked-mineral grains) and the accompanying increase in sulfide content suggest an enrichment mechanism asssociated with reducing conditions in the paleo sea floor.

1. Introduction

The Late Permian (P-Tr) extinction, according to J.J. SEPKOSKI (1982), was the largest in the Phanerozoic. In their more recent arguments for 26-Ma periodicity in extinctions, at least over the last 250 Ma, D.M. RAUP & J.J. SEPKOSKI (1984, 1986) use the P-Tr mass extinction as the oldest datum in their data base (their cornerstone). Before the present study we examined samples from several classic P-Tr sections in South China, where the fossil boundary also is marked by a relatively thin clay bed. Contrary to the claims of several Chinese groups (D. XU et al., 1985; Y. SUN et al., 1985) we have found extremely low Ir concentrations in the "boundary clay" in both their and other localities. The clay in the Chinese sections is mostly illite and contains an unusual trace-element pattern that we generally observe in altered ash from silicic (acidic) volcanic eruptions. Enriched elements include Zr, Cs, Hf, Ta and Th. The siderophiles are depleted; the Ir concentration in the clay is about 1 part per trillion (ppT) or 1×10^{-12} g/g. Some of our South China results and conclusions were reported in D.L. CLARK et al. (1986), and some will be published in the Proceedings of the Snowbird 2 Conference (C.J. ORTH et al., 1991). The Austrian Garnterkofel-1 core, therefore, is of great importance for expanding our knowledge of the P-Tr event and for correlation of the two distant regions.

As part of the collaborative effort to study the Late Permian event in the Gartnerkofel-1 core, we have determined elemental abundances in whole-rock samples. These abundances are used to help elucidate oceanic conditions during deposition and to geochemically characterize this extinction boundary (Text-Fig. 1).

2. Experimental

Radiochemical methods (RNAA) are used to isolate Ir from other competing radionuclides formed during the neutron irradiation of the core (rock) samples. Abundances for about 40 other common and trace elments are determined by instrumental neutron activation analysis (INAA) provided by the Los Alamos Research Reactor Group using their automated system (M.M. MINOR et al., 1981).

Samples for Ir analysis (1 to 2 g) are irradiated for 7 hours in a thermal neutron flux of either 5.7 or 9.7×10^{12} neutrons per cm^2 per sec. After about 1 week of radioactive decay (to allow shorter lived contaminants to decay away), the sample is dissolved with strong acids ($HF + HNO_3 + HClO_4$) in the presence of 20 mg of iridium carrier needed for later chemical-yield determination. Once in solution the sample is put through a radiochemical isolation procedure for Ir that includes two cation exchange resin colums and an Ir-specific precipitation step; the precipitate containing 74-day ^{192}Ir is counted in a high resolution gammy-ray detector and the counts in the 316.5-keV photopeak

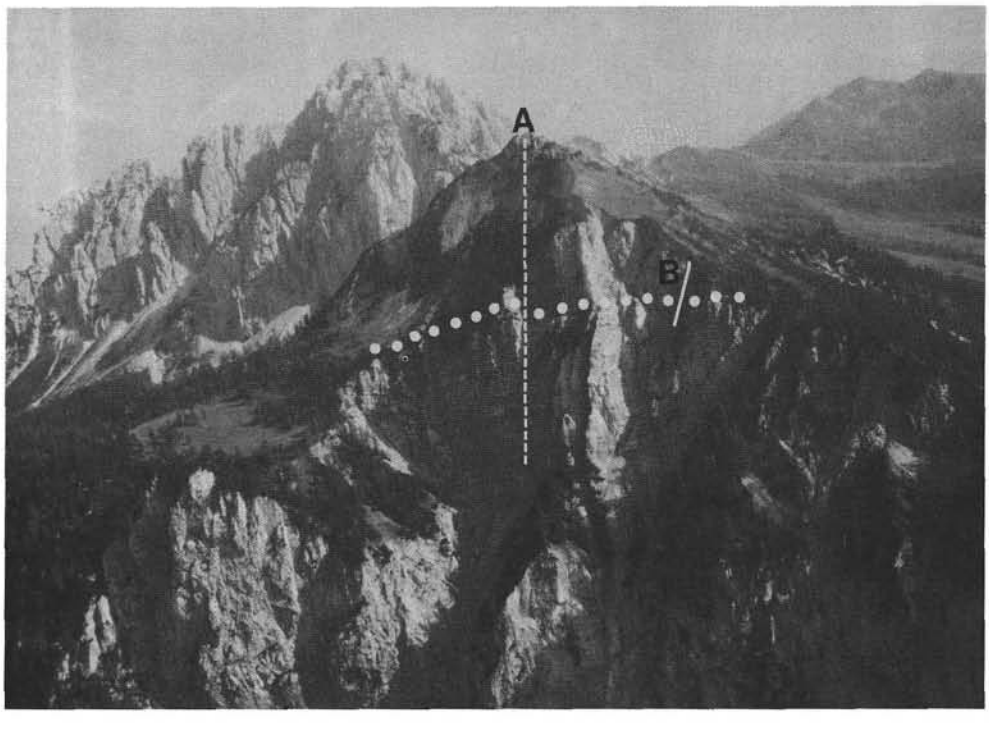

Text-Fig. 1.
Aerial photograph from the north of the Reppwand with the Gartnerkofel (2195 m) in the background.
A: Drill site on Kammleiten (1998 m);
B: Top of the outcrop section.
Dotted line indicates the Permian–Triassic boundary between the Bellerophon Formation (below) and the Werfen Formation above.
Photo: G. FLAJS, Aachen.

are converted into atoms of Ir (abundance). Sensitivity for Ir is about 1 ppT.

The automated INAA system operates as follows:

1) Samples are weighed (3 to 5 g) and loaded in batches of up to 50 into a magazine.
2) Then they are pneumatically transferred into the reactor for 20-sec neutron irradiations at 5×10^{12} neutrons per cm^2 per sec.
3) Followed by immediate counting of delayed neutrons for uranium abundance.
4) Followed by pneumatic transfer to a gamma-ray counter at 20 minutes after the irradiation to determine abundances for short-lived radionuclides such as ^{51}Ti, ^{52}V and ^{56}Mn.
5) The samples are returned (pneumatically) for a second irradiation of 500 sec duration, then stored in a Pb-shielded receiver.
6) After 5 days of radioactive decay samples are returned to the gamma-ray counter to measure radionuclides with intermediate-length half lives such as ^{74}As, ^{99}Mo, ^{122}Sb and ^{140}La.
7) Samples are stored for 2 more weeks, then sent to the gamma-ray counter to measure radionuclides with long half lives, such as ^{46}Sc, ^{60}Co and ^{182}Ta. As with ^{192}Ir, gamma-ray counts are converted to atoms and abundance (concentration by weight).

In a few samples analyses were performed for Ni, Os, Pt and Au. For Ni, about 200 mg of sample are encapsulated in aluminum foil. Six of these and a high purity Ni-foil standard are irradiated in a plastic container for 90 minutes in a special port near the reactor core. This port is lined with boron to remove the thermal (low energy) neutrons. The remaining high energy neutrons induce (n, p) reactions in stable ^{58}Ni to produce ^{58}Co which is counted with a gamma-ray detector. The count rate is then converted to atoms and abundance of Ni. Standard radiochemical procedures not discussed here are used in the determination of the heavy siderophiles, Os, Pt and Au.

3. Results

Whole-rock elemental abundances were measured at Los Alamos for 98 samples from the Gartnerkofel-1 core. Abundances derived from INAA were determined for all the samples, and Ir concentrations were measured on the first 54 (predominantly shales and marls); they are listed in Tables 1 to 5. This group of samples included all of the shaley or marly horizons, mostly one centimeter or less in thickness, in the entire core length. Another batch of 30 samples were predominantly carbonates and their elemental abundances are listed in Tables 6 to 10. These samples bear the same number as that next above in the first group, supplemented by a letter (W.T. HOLSER et al., this volume). Lastly, we received 14 more dolomitic samples that filled in some gaps around the two Ir peaks at

Table 1.
Abundances for Na, Mg, Al, K, Ca, and Sc in the Gartnerkofel-1 core.

Sample (#)	Depth (metres)	Na (ppm)	Mg (%)	Al (%)	K (%)	Ca (%)	Sc (ppm)
12	74.40	1330	4.09	8.23	3.85	5.06	14.50
14	75.90	850	5.78	6.12	3.41	8.93	11.70
15	76.30	725	8.02	4.91	2.38	12.50	9.14
19	82.60	1446	2.73	10.40	5.58	2.30	18.50
25	90.30	1055	6.52	6.56	3.46	9.78	11.40
28	95.30	1159	5.17	6.50	3.43	7.88	13.00
29	95.90	1171	4.97	7.63	3.45	7.15	13.50
31	97.30	1300	5.07	7.55	3.90	7.13	14.60
37	103.78	461	9.20	2.73	1.50	18.40	4.75
44	113.20	402	10.90	1.68	0.97	18.80	2.80
45	114.10	425	11.30	1.85	1.20	18.40	3.28
59	134.53	994	5.99	6.25	3.38	8.36	11.60
66	142.74	582	9.79	2.89	1.51	16.10	5.78
69	146.08	452	11.40	1.85	0.84	19.80	3.10
74	152.57	769	7.78	4.38	3.14	12.70	7.25
81	162.36	640	6.85	4.20	2.78	12.00	6.67
82	163.88	593	8.17	4.16	1.95	12.20	7.17
86	167.98	514	8.20	4.43	2.21	13.60	8.83
100	181.57	1030	4.56	6.02	2.74	9.00	10.20
101	182.00	1003	6.91	5.91	3.16	11.40	9.99
104	182.70	975	7.25	5.43	2.46	12.00	8.43
106	183.51	701	7.91	3.90	2.30	13.10	7.01
112	184.80	565	5.10	4.51	2.96	7.86	6.68
117	185.57	378	0.92	3.38	1.85	0.15	4.65
118	185.65	1710	2.80	10.60	5.38	1.90	18.20
124	186.85	640	9.03	4.25	2.14	14.20	7.22
126	186.97	535	9.01	3.43	2.01	14.30	7.20
127	187.20	1470	2.88	9.00	4.85	3.20	14.10
129	187.55	1138	6.65	6.55	3.34	9.87	11.00
131	188.15	1413	3.12	9.00	4.40	3.20	12.40
133	188.52	337	10.90	1.81	1.32	18.00	2.91
136	189.30	859	8.58	4.03	1.94	14.60	6.53
138	189.80	502	10.33	2.28	1.39	18.60	4.16
143	190.86	1157	6.37	6.97	3.45	9.26	10.10
175	211.85	343	10.54	1.95	0.98	17.30	2.98
185	216.30	386	9.40	2.05	0.81	20.60	3.08
190	220.35	786	6.21	5.54	2.90	10.95	9.32
193	222.20	416	9.39	3.24	1.62	15.70	5.26
196	224.52	593	7.69	3.98	1.72	11.57	6.61
203	229.80	1320	1.91	10.00	4.74	1.75	12.40
204	229.92	128	12.32	0.40	0.18	20.80	0.86
205	230.95	720	7.72	5.08	2.21	13.51	8.40
206	231.25	173	12.10	0.38	0.21	22.70	0.72
207	231.37	125	13.30	0.26	0.14	22.50	0.47
208	231.72	178	12.20	0.54	0.25	20.80	0.99
209	233.08	307	12.30	0.58	0.28	21.20	1.02
232	259.50	947	9.48	5.33	2.10	14.40	10.40
236	263.54	1213	6.21	8.21	3.74	8.22	12.80
238	266.80	494	11.00	2.37	1.16	18.40	4.28
262	292.30	1530	4.12	10.70	5.82	3.62	16.70
265	294.80	1099	7.54	7.34	3.42	10.90	12.40
267	295.95	581	10.41	3.22	1.57	16.50	7.22
284	314.86	576	9.30	3.99	2.12	15.80	6.17
286	315.52	1740	2.30	13.10	6.59	0.24	22.30
(+/- %)	--	10	15	10	20	12	10

Table 2.
Abundances for Ti, V, Cr, Mn, Fe, and Co in the Gartnerkofel-1 core.

Sample (#)	Depth (metres)	Ti (ppm)	V (ppm)	Cr (ppm)	Mn (ppm)	Fe (%)	Co (ppm)
12	74.40	4980	96	75	181	2.3	15.4
14	75.90	2950	73	62	282	2.9	7.2
15	76.30	2330	66	42	290	2.0	9.1
19	82.60	4050	107	103	217	3.4	17.8
25	90.30	3660	80	59	248	1.8	7.8
28	95.30	3230	84	67	284	2.6	13.6
29	95.90	3290	96	68	292	2.6	18.4
31	97.30	3740	94	75	174	2.1	12.7
37	103.78	1300	35	38	263	1.2	5.2
44	113.20	1010	25	27	144	0.7	3.3
45	114.10	1660	24	22	150	0.7	2.7
59	134.53	3650	83	62	94	1.7	16.3
66	142.74	1790	31	30	143	1.1	5.7
69	146.08	1140	19	28	141	0.7	4.4
74	152.57	2610	53	44	155	1.1	9.1
81	162.36	2860	41	44	184	1.5	12.5
82	163.88	3100	47	39	178	1.4	12.3
86	167.98	3070	50	52	100	0.7	3.6
100	181.57	3440	70	73	246	1.7	12.1
101	182.00	3070	72	55	205	1.8	9.2
104	182.70	3760	70	53	164	1.7	13.3
106	183.51	2840	44	45	197	2.2	10.0
112	184.80	2010	73	54	149	5.1	25.2
117	185.57	1860	120	35	50	24.6	29.9
118	185.65	5700	133	104	117	2.9	23.6
124	186.85	2500	51	39	161	1.3	10.9
126	186.97	1280	38	26	160	1.0	6.5
127	187.20	5190	117	103	117	3.0	9.9
129	187.55	4770	80	86	131	2.1	13.3
131	188.15	5760	124	96	80	2.7	28.3
133	188.52	880	22	20	104	0.6	2.6
136	189.30	1490	42	37	100	1.2	5.1
138	189.80	750	28	17	95	0.6	1.5
143	190.86	5250	92	77	107	2.6	14.4
175	211.85	1170	21	19	109	0.8	3.1
185	216.30	1120	23	31	322	1.2	4.5
190	220.35	2690	79	51	202	1.8	11.0
193	222.20	1890	54	34	233	2.8	15.5
196	224.52	2680	63	54	208	3.9	14.2
203	229.80	8400	136	140	54	3.0	8.3
204	229.92	400	8	6	106	0.5	1.6
205	230.95	2870	133	108	113	2.5	7.9
206	231.25	400	11	7	118	3.9	0.7
207	231.37	400	7	11	110	0.4	0.9
208	231.72	400	8	8	102	0.4	1.2
209	233.08	500	16	9	79	0.4	1.0
232	259.50	3110	75	84	102	1.0	5.6
236	263.54	4120	88	98	75	1.8	6.2
238	266.80	930	28	28	100	0.7	3.4
262	292.30	5930	118	113	62	3.4	13.4
265	294.80	3740	61	72	76	1.7	8.9
267	295.95	1220	29	27	117	0.9	3.5
284	314.86	2040	51	54	154	1.3	5.2
286	315.52	6010	208	138	44	2.8	6.3
(+/- %)	--	15	12	12	10	16	10

Sample (#)	Depth (metres)	As (ppm)	Rb (ppm)	Sb (ppm)	Cs (ppm)	Ba (ppm)	La (ppm)
12	74.40	12.6	167	1.7	37.0	470	46.2
14	75.90	3.9	132	1.2	22.0	320	26.5
15	76.30	11.3	94	1.6	17.0	240	24.8
19	82.60	9.8	186	2.1	35.0	520	34.1
25	90.30	10.1	107	1.1	14.0	370	33.7
28	95.30	15.9	165	1.1	16.4	310	30.0
29	95.90	10.4	133	1.5	16.0	450	35.7
31	97.30	10.1	152	0.4	22.0	390	31.8
37	103.78	4.1	50	0.3	5.5	170	10.9
44	113.20	3.7	26	0.3	4.0	90	9.6
45	114.10	4.8	32	0.4	3.5	80	10.9
59	134.53	20.8	109	1.2	12.3	450	33.0
66	142.74	5.3	55	0.4	6.0	140	14.7
69	146.08	3.1	32	0.2	3.5	95	8.4
74	152.57	8.9	68	0.6	6.7	300	22.5
81	162.36	19.5	60	0.9	6.4	305	25.7
82	163.88	17.3	69	0.8	7.0	210	22.3
86	167.98	3.1	73	0.2	6.5	230	21.0
100	181.57	16.3	98	0.8	11.6	450	30.3
101	182.00	13.5	101	0.7	12.5	270	24.5
104	182.70	18.7	91	0.6	10.0	250	26.4
106	183.51	28.7	84	0.8	7.9	250	18.9
112	184.80	100.0	78	2.3	10.9	220	18.6
117	185.57	239.0	110	8.2	7.8	280	17.9
118	185.65	43.2	206	2.5	25.5	420	46.8
124	186.85	8.9	88	0.5	8.7	130	16.8
126	186.97	7.7	52	0.4	7.9	140	15.4
127	187.20	22.6	160	1.4	20.3	400	46.3
129	187.55	25.8	128	1.9	11.6	380	34.6
131	188.15	55.2	186	5.6	15.6	450	38.7
133	188.52	3.6	31	0.3	3.4	100	9.1
136	189.30	7.3	68	0.5	7.1	190	15.1
138	189.80	2.4	36	0.2	3.3	90	7.7
143	190.86	89.0	125	5.8	11.9	330	33.3
175	211.85	6.7	46	0.4	3.4	130	12.1
185	216.30	5.8	31	0.2	3.1	90	9.8
190	220.35	30.3	106	1.4	9.9	210	25.6
193	222.20	45.3	59	1.6	6.5	140	16.5
196	224.52	84.5	74	2.9	7.2	350	26.9
203	229.80	49.5	164	2.1	16.0	410	66.5
204	229.92	9.1	13	0.2	7.1	60	8.6
205	230.95	44.6	96	2.3	10.1	230	25.5
206	231.25	1.9	8	0.2	0.9	40	4.5
207	231.37	2.0	5	0.2	0.3	30	3.7
208	231.72	1.6	5	0.1	1.1	28	3.6
209	233.08	1.6	5	0.2	1.1	29	3.3
232	259.50	7.2	115	1.5	19.0	740	16.8
236	263.54	14.6	163	1.9	21.0	320	27.1
238	266.80	4.8	63	0.6	9.5	150	9.0
262	292.30	47.1	249	5.9	31.0	305	22.0
265	294.80	28.5	76	2.8	20.0	230	14.0
267	295.95	3.0	58	0.5	10.4	120	10.0
284	314.86	9.9	77	1.3	10.0	150	12.0
286	315.52	38.5	355	5.8	47.0	1170	35.0
(+/- %)	--	10	20	15	15	20	10

Table 3.
Abundances for As, Rb, Sb, Cs, Ba, and La in the Gartnerkofel-1 core.

←

Sample (#)	Depth (metres)	Ce (ppm)	Sm (ppm)	Eu (ppm)	Tb (ppm)	Dy (ppm)	Yb (ppm)
12	74.40	68.0	7.6	1.2	0.7	4.1	2.5
14	75.90	59.0	4.6	1.0	0.6	3.0	1.8
15	76.30	38.0	5.5	1.0	0.5	3.6	1.4
19	82.60	58.0	4.8	0.9	0.4	3.8	2.3
25	90.30	53.0	5.8	0.9	0.5	11.8	1.7
28	95.30	68.0	5.3	1.2	0.6	6.9	2.4
29	95.90	58.0	6.6	1.2	0.6	4.9	2.2
31	97.30	73.0	5.7	1.1	0.7	4.0	2.3
37	103.78	18.0	1.9	0.4	0.1	0.8	0.9
44	113.20	16.2	1.5	0.3	0.2	1.3	0.8
45	114.10	16.6	2.0	0.3	0.2	1.2	0.7
59	134.53	48.0	5.1	0.9	0.5	3.8	2.2
66	142.74	30.0	2.2	0.5	0.2	2.0	1.2
69	146.08	13.6	1.4	0.3	0.2	1.1	0.5
74	152.57	38.0	4.0	0.6	0.1	2.6	1.7
81	162.36	47.0	5.0	0.8	0.5	3.9	1.9
82	163.88	37.0	3.8	0.7	0.3	5.6	1.2
86	167.98	40.0	2.6	0.5	0.3	6.7	1.7
100	181.57	55.0	5.3	1.1	0.5	5.4	2.2
101	182.00	39.0	3.4	0.5	0.1	2.0	1.6
104	182.70	38.0	3.9	0.7	0.2	1.5	1.2
106	183.51	39.0	2.7	0.5	0.2	1.6	1.5
112	184.80	32.0	2.3	0.5	0.2	1.7	1.2
117	185.57	28.0	3.4	0.6	0.3	2.0	0.9
118	185.65	80.0	7.0	1.2	0.7	4.1	2.4
124	186.85	27.0	0.9	0.5	0.3	1.6	1.2
126	186.97	29.0	2.1	0.5	0.3	1.4	1.1
127	187.20	70.0	5.2	1.1	0.7	4.2	2.5
129	187.55	61.0	3.6	0.6	0.5	2.8	2.1
131	188.15	63.0	3.2	0.7	0.5	3.2	2.3
133	188.52	16.6	1.2	0.2	0.2	0.9	0.6
136	189.30	28.0	1.9	0.4	0.2	1.6	0.9
138	189.80	13.3	1.3	0.3	0.2	0.8	0.5
143	190.86	49.0	2.6	0.7	0.3	2.4	2.3
175	211.85	24.0	1.5	0.4	0.2	1.8	1.0
185	216.30	14.3	1.1	0.3	0.1	0.7	0.5
190	220.35	44.0	4.7	0.8	0.2	3.2	1.8
193	222.20	32.0	2.0	0.6	0.4	2.5	1.4
196	224.52	55.0	2.4	0.7	0.5	2.8	1.7
203	229.80	76.0	3.4	0.8	0.7	3.8	2.8
204	229.92	8.8	1.6	0.4	0.2	1.3	0.6
205	230.95	48.3	2.7	0.6	0.5	2.3	1.9
206	231.25	6.2	0.8	0.2	0.1	1.0	0.2
207	231.37	5.1	0.7	0.1	0.1	1.0	0.2
208	231.72	4.9	0.7	0.1	0.1	1.5	0.2
209	233.08	6.7	0.7	0.2	0.1	1.4	0.3
232	259.50	29.0	1.7	0.5	0.4	2.3	1.3
236	263.54	51.0	2.7	0.6	0.5	2.7	1.8
238	266.80	16.0	1.3	0.3	0.1	1.2	0.7
262	292.30	41.0	3.2	0.6	0.5	2.6	1.7
265	294.80	26.0	1.8	0.5	0.4	2.0	1.2
267	295.95	18.0	1.3	0.4	0.2	1.4	0.8
284	314.86	23.0	1.7	0.5	0.3	1.8	1.2
286	315.52	68.0	5.3	1.0	0.6	4.2	2.6
(+/- %)	--	15	12	15	25	10	15

Table 4.
Abundances for Ce, Sm, Eu, Tb, Dy, and Yb in the Gartnerkofel-1 core.

←

Sample (#)	Depth (metres)	Lu (ppm)	Hf (ppm)	Ta (ppm)	Ir (ppT)	Th (ppm)	U (ppm)
12	74.40	0.31	4.2	1.3	29	13.5	3.7
14	75.90	0.29	2.4	0.7	12	8.9	1.7
15	76.30	0.22	1.7	0.6	13	6.1	2.7
19	82.60	0.23	3.2	1.1	34	11.2	3.6
25	90.30	0.22	2.5	0.8	29	8.5	11.8
28	95.30	0.37	2.8	0.8	37	9.2	6.9
29	95.90	0.29	3.2	0.9	26	8.9	5.6
31	97.30	0.38	3.7	1.0	57	11.9	4.1
37	103.78	0.13	1.2	0.4	11	2.9	3.3
44	113.20	0.08	1.0	0.3	7	2.5	1.8
45	114.10	0.09	1.5	0.5	8	2.5	2.2
59	134.53	0.26	4.0	1.0	52	11.6	17.8
66	142.74	0.15	1.6	0.5	11	5.2	5.5
69	146.08	0.06	0.6	0.2	11	2.1	2.9
74	152.57	0.20	3.3	0.6	12	6.4	5.4
81	162.36	0.26	5.0	0.9	12	7.4	3.1
82	163.88	0.24	2.6	0.5	21	6.1	5.6
86	167.98	0.23	3.8	0.8	33	9.5	6.7
100	181.57	0.32	3.4	1.0	22	8.6	4.1
101	182.00	0.21	2.4	0.7	34	7.4	3.6
104	182.70	0.17	2.9	0.9	36	7.1	4.4
106	183.51	0.21	3.2	0.8	35	7.8	4.5
112	184.80	0.16	2.4	0.5	95	7.3	6.9
117	185.57	0.17	1.8	0.4	233	9.6	4.4
118	185.65	0.37	4.0	1.5	31	15.2	4.1
124	186.85	0.13	1.9	0.6	28	5.4	4.2
126	186.97	0.13	1.4	0.3	41	4.5	3.6
127	187.20	0.36	4.3	1.2	86	14.7	11.3
129	187.55	0.26	5.5	1.4	68	10.7	9.2
131	188.15	0.35	6.8	1.5	100	13.0	10.5
133	188.52	0.11	1.2	0.4	7	2.9	2.2
136	189.30	0.13	1.8	0.5	16	5.2	3.9
138	189.80	0.09	1.0	0.3	23	2.9	2.5
143	190.86	0.25	4.2	1.2	83	10.7	11.0
175	211.85	0.16	2.1	0.3	11	4.1	3.4
185	216.30	0.08	0.9	0.3	17	2.6	2.9
190	220.35	0.23	2.9	0.8	26	6.6	4.7
193	222.20	0.15	1.8	0.5	74	4.8	5.3
196	224.52	0.33	5.2	1.0	165	10.5	12.0
203	229.80	0.59	9.4	2.3	116	16.6	20.9
204	229.92	0.07	0.4	0.1	5	0.8	1.4
205	230.95	0.30	4.1	0.8	47	10.0	10.2
206	231.25	0.02	0.1	0.1	2	0.5	1.9
207	231.37	0.03	0.1	0.1	3	0.3	1.7
208	231.72	0.03	0.1	0.3	6	0.7	1.8
209	233.08	0.04	0.2	0.3	7	0.8	3.4
232	259.50	0.17	3.5	1.1	14	7.7	12.7
236	263.54	0.31	4.5	1.2	30	11.9	10.6
238	266.80	0.13	0.6	0.3	10	2.8	9.9
262	292.30	0.30	4.7	1.5	29	12.8	18.3
265	294.80	0.21	3.5	1.3	16	10.3	17.9
267	295.95	0.10	0.9	0.4	14	3.5	12.1
284	314.86	0.12	1.5	0.5	15	4.7	13.5
286	315.52	0.41	5.4	1.9	34	16.6	19.6
(+/- %)	--	20	12	20	10	12	7

Table 5.
Abundances for Lu, Hf, Ta, Ir, Th, and U in the Gartnerkofel-1 core.

Table 6.
Abundances for Na, Mg, Al, K, Ca, and Sc in the Gartner-kofel-1 core.

Sample (#)	Depth (metres)	Na (ppm)	Mg (%)	Al (%)	K (%)	Ca (%)	Sc (ppm)
1901	220.02	320	8.8	1.49	0.93	18.3	2.80
1902	220.17	340	7.6	1.66	1.00	17.6	2.40
1903	220.75	430	7.2	2.90	1.62	13.7	4.50
1911	220.90	290	10.4	1.37	0.78	18.8	2.20
1912	221.40	340	8.4	1.83	1.12	16.9	3.00
1913	221.73	450	6.9	2.20	1.41	15.5	3.40
1914	221.85	520	6.8	2.60	1.57	13.2	4.00
1915	222.01	350	9.7	1.77	1.06	16.8	2.70
1916	222.28	460	8.0	2.37	1.47	15.4	4.20
1921	222.50	250	9.2	1.16	0.59	19.7	2.00
1931	223.30	130	9.9	0.46	0.20	19.0	0.99
1941	223.65	190	12.0	0.64	0.36	20.7	1.10
1942	223.85	200	10.1	0.83	0.44	20.5	1.50
1943	224.00	290	8.0	1.29	0.67	18.9	2.10
1944	224.77	180	9.7	0.43	0.20	19.0	0.82
1945	224.90	150	12.1	0.44	0.21	20.7	0.84
1951	224.77	270	9.5	1.17	0.56	19.1	2.10
1952	224.90	250	8.6	1.12	0.52	19.8	1.70
1962	225.24	93	11.0	0.17	0.06	21.0	0.24
1963	225.55	150	12.9	0.32	0.18	21.5	0.65
1982	227.20	102	11.5	0.04	0.02	22.0	0.07
1983	227.50	117	9.4	0.09	0.03	21.3	0.20
1991	228.35	160	11.0	0.04	0.02	20.0	0.09
1992	228.66	133	13.2	0.04	0.02	21.5	0.09
1993	229.40	100	11.4	0.03	0.02	22.1	0.09
2011	229.78	100	9.4	0.05	0.03	20.8	0.08
2021	229.98	148	10.0	0.57	0.27	19.0	0.92
2041	230.33	173	12.4	0.66	0.33	20.9	1.30
2042	230.54	138	10.9	0.40	0.17	21.5	0.93
2043	230.78	164	9.1	0.24	0.13	20.7	0.52
(+/- %)	--	10	15	20	25	12	20

Last digit in sample # corresponds to a letter. For example, 1 is A and 4 is D. Sample # 1945 is 194E.

Table 7.
Abundances for Ti, V, Cr, Mn, Fe, and Co in the Gartner-kofel-1 core.

Sample (#)	Depth (metres)	Ti (ppm)	V (ppm)	Cr (ppm)	Mn (ppm)	Fe (%)	Co (ppm)
1901	220.02	700	22	12	223	0.85	2.7
1902	220.17	850	25	13	210	0.76	3.0
1903	220.75	1900	34	24	196	0.98	3.8
1911	220.90	800	17	12	206	0.72	4.1
1912	221.40	860	25	16	203	0.81	3.4
1913	221.73	1500	27	22	186	0.82	4.4
1914	221.85	1400	28	23	175	0.82	4.0
1915	222.01	1000	22	16	190	0.74	4.2
1916	222.28	1400	29	21	191	0.89	3.7
1921	222.50	610	18	11	202	1.17	3.0
1931	223.30	300	8	5	209	0.49	1.4
1941	223.65	320	10	8	202	0.52	2.6
1942	223.85	760	10	7	189	0.52	1.1
1943	224.00	760	16	12	196	0.55	1.9
1944	224.77	500	7	4	190	0.41	0.8
1945	224.90	410	7	5	193	0.47	2.4
1951	224.77	870	11	13	200	0.57	1.8
1952	224.90	800	20	12	221	0.77	3.9
1962	225.24	150	2	2	170	0.37	0.4
1963	225.55	400	6	4	162	0.43	2.1
1982	227.20	80	1	1	153	0.40	0.3
1983	227.50	160	2	2	113	0.27	1.0
1991	228.35	90	1	1	123	0.29	0.3
1992	228.66	90	1	1	138	0.33	1.9
1993	229.40	95	1	1	118	0.31	0.3
2011	229.78	80	1	2	125	0.27	0.9
2021	229.98	360	8	6	98	0.33	0.8
2041	230.33	410	8	8	105	0.44	2.4
2042	230.54	360	5	4	95	0.31	0.7
2043	230.78	200	5	4	88	0.31	1.2
(+/- %)	--	25	20	20	10	16	20

Last digit in sample # corresponds to a letter. For example, 2 is B and 3 is C. Sample # 1901 is 190A.

Table 8.
Abundances for As, Rb, Sb, Cs, Ba, and La in the Gartner-kofel-1 core.

Sample (#)	Depth (metres)	As (ppm)	Rb (ppm)	Sb (ppm)	Cs (ppm)	Ba (ppm)	La (ppm)
1901	220.02	7.10	29	0.35	3.00	90	8.7
1902	220.17	5.70	24	0.40	3.00	100	9.0
1903	220.75	7.40	48	0.38	4.70	100	13.4
1911	220.90	4.70	21	0.30	2.60	102	7.6
1912	221.40	6.90	43	0.41	3.20	110	10.3
1913	221.73	7.20	36	0.33	3.60	110	12.4
1914	221.85	7.40	52	0.33	4.40	180	13.8
1915	222.01	5.50	29	0.36	2.80	120	9.9
1916	222.28	8.60	51	0.50	4.40	190	13.7
1921	222.50	21.00	15	0.66	1.70	110	7.2
1931	223.30	2.60	4	0.10	0.71	60	4.2
1941	223.65	2.20	11	0.12	1.00	70	5.1
1942	223.85	2.90	16	0.14	1.40	70	6.1
1943	224.00	3.60	19	0.17	2.20	100	9.0
1944	224.77	2.10	7	0.04	0.78	90	3.7
1945	224.90	3.30	10	0.04	0.72	60	4.2
1951	224.77	3.20	19	0.14	1.90	70	7.7
1952	224.90	6.70	13	0.31	1.80	80	7.3
1962	225.24	0.86	50	0.07	0.20	50	1.4
1963	225.55	2.40	7	0.14	0.40	60	2.1
1982	227.20	0.43	2	0.03	0.09	30	0.6
1983	227.50	1.70	2	0.11	0.30	50	2.4
1991	228.35	0.22	2	0.01	0.08	30	1.4
1992	228.66	0.50	2	0.04	0.08	30	1.1
1993	229.40	0.33	1	0.03	0.07	25	1.1
2011	229.78	0.21	2	0.02	0.08	30	1.7
2021	229.98	1.90	8	0.13	0.75	40	9.3
2041	230.33	4.80	12	0.18	1.20	62	10.2
2042	230.54	1.60	8	0.10	0.54	40	9.3
2043	230.78	2.10	3	0.05	0.35	70	6.7
(+/- %)	--	20	25	25	20	30	15

Last digit in sample # corresponds to a letter. For example, 1 is A and 6 is F. Sample # 1916 is 191F.

Table 9.
Abundances for Ce, Sm, Eu, Tb, Dy, and Yb in the Gartner-kofel-1 core.

Sample (#)	Depth (metres)	Ce (ppm)	Sm (ppm)	Eu (ppm)	Tb (ppm)	Dy (ppm)	Yb (ppm)
1901	220.02	16.2	1.70	0.35	0.25	1.80	0.76
1902	220.17	16.5	1.50	0.30	0.18	1.30	0.80
1903	220.75	23.1	2.20	0.40	0.22	2.00	1.10
1911	220.90	15.6	1.60	0.35	0.23	1.60	0.66
1912	221.40	19.6	1.90	0.38	0.28	1.90	0.88
1913	221.73	24.1	2.10	0.42	0.28	2.30	1.20
1914	221.85	24.8	2.30	0.43	0.35	2.20	1.20
1915	222.01	18.6	1.70	0.34	0.21	2.00	0.88
1916	222.28	27.3	2.50	0.51	0.30	2.50	1.30
1921	222.50	16.5	1.50	0.29	0.25	1.20	0.55
1931	223.30	9.0	0.96	0.19	0.10	0.80	0.42
1941	223.65	10.4	0.97	0.19	0.14	0.80	0.36
1942	223.85	11.7	1.10	0.25	0.12	1.00	0.62
1943	224.00	18.5	1.60	0.34	0.13	1.90	0.75
1944	224.77	8.0	0.80	0.16	0.11	0.53	0.24
1945	224.90	8.7	0.80	0.17	0.11	0.80	0.27
1951	224.77	15.0	1.30	0.30	0.21	1.20	0.76
1952	224.90	13.4	1.30	0.24	0.11	1.10	0.66
1962	225.24	2.3	0.24	0.07	0.02	0.40	0.08
1963	225.55	4.8	0.46	0.09	0.03	0.50	0.16
1982	227.20	0.9	0.14	0.02	0.03	0.20	0.13
1983	227.50	2.5	0.47	0.08	0.08	0.60	0.25
1991	228.35	1.4	0.24	0.06	0.06	0.30	0.19
1992	228.66	1.1	0.24	0.06	0.06	0.30	0.17
1993	229.40	1.4	0.17	0.04	0.04	0.20	0.16
2011	229.78	1.5	0.49	0.10	0.06	0.40	0.23
2021	229.98	10.5	1.70	0.34	0.21	1.30	0.65
2041	230.33	12.5	1.80	0.35	0.23	1.70	0.64
2042	230.54	10.1	1.70	0.34	0.25	1.80	0.82
2043	230.78	6.7	1.00	0.22	0.16	1.20	0.50
(+/- %)	--	20	17	20	35	20	22

Last digit in sample # corresponds to a letter. For example, 1 is A and 2 is B. Sample # 2042 is 204B.

Table 10.
Abundances for Lu, Hf, Ta, Ir, Th, and U in the Gartnerkofel-1 core.

Sample (#)	Depth (metres)	Lu (ppm)	Hf (ppm)	Ta (ppm)	Th (ppm)	U (ppm)
1901	220.02	0.11	0.59	0.32	2.10	1.56
1902	220.17	0.08	0.96	0.29	2.50	1.57
1903	220.75	0.16	1.90	0.39	4.30	2.86
1911	220.90	0.10	1.10	0.26	2.30	1.46
1912	221.40	0.13	1.40	0.35	3.10	1.99
1913	221.73	0.15	2.30	0.42	4.20	2.45
1914	221.85	0.16	2.70	0.41	4.50	2.78
1915	222.01	0.13	1.90	0.37	3.20	1.87
1916	222.28	0.18	2.10	0.35	4.10	2.49
1921	222.50	0.05	0.46	0.10	2.00	2.13
1931	223.30	0.05	0.25	0.10	1.10	1.11
1941	223.65	0.05	0.68	0.10	1.30	1.13
1942	223.85	0.08	0.95	0.19	1.50	1.28
1943	224.00	0.11	1.30	0.23	2.10	2.09
1944	224.77	0.05	0.37	0.10	0.84	1.03
1945	224.90	0.06	0.62	0.08	0.94	1.17
1951	224.77	0.08	1.20	0.16	2.50	1.87
1952	224.90	0.09	0.66	0.08	1.80	1.84
1962	225.24	0.03	0.08	0.01	0.23	0.88
1963	225.55	0.03	0.21	0.03	0.45	1.24
1982	227.20	0.03	0.03	0.01	0.10	0.59
1983	227.50	0.05	0.06	0.01	0.13	0.80
1991	228.35	0.02	0.03	0.01	0.06	0.71
1992	228.66	0.03	0.03	0.01	0.07	0.65
1993	229.40	0.02	0.04	0.01	0.06	0.55
2011	229.78	0.04	0.03	0.04	0.06	0.41
2021	229.98	0.07	0.39	0.11	0.85	1.41
2041	230.33	0.11	0.51	0.15	1.20	1.81
2042	230.54	0.09	0.27	0.08	0.72	1.37
2043	230.78	0.08	0.18	0.05	0.46	1.19
(+/- %)	--	25	20	35	20	10

Last digit in sample # corresponds to a letter. For example, 3 is C and 5 is E. Sample # 1914 is 191D

Table 11.
Abundances for Na, Mg, Al, K, Ca, and Sc in the Gartnerkofel-1 core.

Sample (#)	Depth (metres)	Na (ppm)	Mg (%)	Al (%)	K (%)	Ca (%)	Sc (ppm)
108	183.97	256	10.30	0.73	0.48	20.9	1.27
110	184.43	175	9.03	0.41	0.25	21.4	0.71
113	184.96	207	9.90	0.72	0.43	20.3	1.29
114	185.26	217	12.30	0.75	0.44	20.2	1.47
115	185.30	216	10.20	0.80	0.53	20.4	1.37
116	185.51	199	8.72	0.69	0.47	20.1	1.37
118	185.69	330	11.30	1.42	0.90	19.4	2.94
119	185.96	478	8.07	2.56	1.87	15.7	4.60
120	186.15	262	8.21	1.04	0.58	19.2	1.93
122	186.77	173	9.90	0.88	0.30	20.0	1.66
194	222.35	185	12.70	0.37	0.12	21.7	0.71
195	223.94	202	10.00	0.78	0.34	20.5	1.40
197	225.40	124	9.38	0.20	0.09	21.0	0.33
198	226.00	71	10.80	0.08	0.04	20.7	0.17
(+/- %)	--	10	15	20	25	12	20

Table 12.
Abundances for Ti, V, Cr, Mn, Fe, and Co in the Gartnerkofel-1 core.

Sample (#)	Depth (metres)	Ti (ppm)	V (ppm)	Cr (ppm)	Mn (ppm)	Fe (%)	Co (ppm)
108	183.97	600	10	8.2	161	0.51	0.6
110	184.43	350	6	7.6	163	0.48	1.8
113	184.96	600	12	8.8	161	0.52	1.2
114	185.26	500	11	8.3	165	0.58	2.8
115	185.30	590	10	8.0	169	0.59	1.3
116	185.51	620	13	10.0	208	1.02	2.2
118	185.69	770	22	16.0	200	0.90	4.1
119	185.96	1580	30	25.0	208	1.25	4.6
120	186.15	750	10	14.0	224	0.69	1.9
122	186.77	650	11	12.0	179	0.60	1.8
194	222.35	300	5	5.8	221	0.53	0.7
195	223.94	530	10	9.0	197	0.51	1.4
197	225.40	200	3	4.8	147	0.32	1.2
198	226.00	100	1	2.8	153	0.42	0.3
(+/- %)	--	30	25	20	10	16	30

Table 13.
Abundances for As, Rb, Sb, Cs, Ba, and La in the Gartnerkofel-1 core.

Sample (#)	Depth (metres)	As (ppm)	Rb (ppm)	Sb (ppm)	Cs (ppm)	Ba (ppm)	La (ppm)
108	183.97	1.20	16	0.04	1.40	80	4.44
110	184.43	3.00	5	0.03	0.85	45	2.94
113	184.96	1.60	15	0.04	1.50	75	3.92
114	185.26	1.70	12	0.10	1.60	80	4.72
115	185.30	1.60	14	0.08	1.50	140	5.23
116	185.51	6.50	21	0.34	1.40	75	6.63
118	185.69	5.50	29	0.34	3.50	78	9.51
119	185.96	8.20	52	0.34	5.10	153	15.20
120	186.15	2.10	23	0.10	2.10	90	6.91
122	186.77	2.00	18	0.09	1.90	100	5.84
194	222.35	1.60	6	0.04	0.72	110	4.05
195	223.94	2.90	21	0.18	1.10	95	6.02
197	225.40	0.59	9	0.06	0.22	50	1.73
198	226.00	0.73	4	0.04	0.11	20	1.00
(+/- %)	--	20	25	25	20	30	15

Table 14.
Abundances for Ce, Sm, Eu, Tb, Dy, and Yb in the Gartnerkofel-1 core.

Sample (#)	Depth (metres)	Ce (ppm)	Sm (ppm)	Eu (ppm)	Tb (ppm)	Dy (ppm)	Yb (ppm)
108	183.97	8.6	0.87	0.18	0.09	0.72	0.34
110	184.43	6.1	0.55	0.11	0.04	0.40	0.28
113	184.96	8.5	0.75	0.16	0.11	0.68	0.28
114	185.26	10.0	0.99	0.20	0.13	0.90	0.36
115	185.30	9.5	1.00	0.21	0.15	0.92	0.33
116	185.51	14.2	1.42	0.28	0.25	1.20	0.64
118	185.69	20.4	1.75	0.38	0.23	1.44	0.79
119	185.96	29.0	2.75	0.50	0.27	2.22	1.29
120	186.15	14.0	1.28	0.25	0.16	2.70	0.56
122	186.77	12.0	1.08	0.24	0.10	1.10	0.50
194	222.35	9.0	0.89	0.19	0.10	1.00	0.40
195	223.94	11.8	1.13	0.22	0.19	1.50	0.49
197	225.40	4.0	0.33	0.06	0.08	0.50	0.21
198	226.00	1.7	0.17	0.04	0.04	0.30	0.12
(+/- %)	--	20	17	20	35	20	22

Table 15.
Abundances for Lu, Hf, Ta, Ir, Th, and U in the Gartnerkofel-1 core.

Sample (#)	Depth (metres)	Lu (ppm)	Hf (ppm)	Ta (ppm)	Ir (ppT)	Th (ppm)	U (ppm)
108	183.97	0.05	0.37	0.10	3.9	1.0	1.00
110	184.43	0.04	0.20	0.05	5.5	0.6	0.71
113	184.96	0.04	0.35	0.10	4.9	1.1	1.15
114	185.26	0.06	0.26	0.11	5.8	1.1	1.06
115	185.30	0.06	0.44	0.10	6.5	1.4	1.09
116	185.51	0.09	0.30	0.08	11.0	1.3	0.96
118	185.69	0.12	0.66	0.23	0.0	2.3	1.23
119	185.96	0.18	2.00	0.32	13.0	4.5	2.17
120	186.15	0.07	0.60	0.20	0.0	1.9	1.00
122	186.77	0.07	0.42	0.13	0.0	1.3	1.41
194	222.35	0.05	0.39	0.10	3.0	1.0	0.95
195	223.94	0.07	0.64	0.12	22.0	1.5	1.33
197	225.40	0.02	0.11	0.06	4.0	0.3	1.09
198	226.00	0.01	0.06	0.03	2.5	0.2	0.77
(+/- %)	--	25	20	35	15	20	10

Table 16.
Abundances for Ni, Au, Pt, and Os in the Gartnerkofel-1 core.

Sample (#)	Depth (m)	Ni (ppm)	Au (ppb)	Pt (ppb)	Os (ppb)
110	184.43	7.2	---	---	---
112	184.80	7.3	5.3	< 1	---
115	185.30	7.8	---	---	---
116	185.51	11.7	---	---	---
117	185.57	110	3.7	< 1	0.31
118	185.69	48	0.94	< 1	---
190	220.35	43	---	---	---
195	223.94	7.2	---	---	---
196	224.52	107	---	---	---
197	225.40	6.0	---	---	---

185.57 and 224.5 meters and the data for these, including some Ir assays, are listed in Tables 11 to 15. In the tables, elements are listed in order of increasing atomic number, with six elements per table. A number of elements usually measured by INAA techniques are not reported because their abundances in many samples were below detection limits (e. g. Cu, Zn, Se, Br, Zr, Mo, Ag, and Au). The uncertainties shown at the bottom of each of the columns represent our best estimates at the 95 % confidence level for an average sample. In samples where a particular abundance is very low the uncertainty could be considerably larger than the value listed for that element.

Data for the few analyses of Ni, Os, Pt and Au are listed separately in Table 16.

A limited number of analyses, including Ir, were made of samples from a 5-m section of the Reppwand outcrop, and these are listed in Tables 17 to 21; these data are not illustrated by figures.

Sample No.	Cumulative thickness*) [m]	Thickness [m]	Na [ppm]	Mg [%]	Al [%]	K [%]	Ca [%]	Sc [ppm]
86462	5.09	0.02	810	7.1	5.13	2.65	10.8	8.36
86460	4.37	0.001	795	7.6	4.31	2.22	12.7	7.50
86459C	4.23	0.02	239	10.8	1.09	0.54	18.2	2.00
86459B	4.21	0.02	224	11.6	0.91	0.50	20.0	1.74
86459A	4.19	0.02	250	11.6	1.04	0.63	19.4	2.24
86458	4.17	0.003	845	2.6	6.78	3.54	1.6	9.21
86456D	4.08	0.02	260	11.6	0.85	0.50	19.1	1.52
86456C	4.05	0.02	244	10.9	0.88	0.44	19.3	1.32
86456B	4.03	0.02	221	11.5	0.72	0.32	20.0	1.14
86456A	4.01	0.02	234	11.5	0.81	0.47	19.3	1.40
86455	3.99	0.001	820	6.3	5.32	2.63	9.2	7.65
86457E	3.96	0.02	113	13.3	0.22	0.11	21.8	0.41
86457D	3.93	0.02	96	12.4	0.19	0.07	20.8	0.36
86457C	3.91	0.02	95	12.4	1.73	0.07	20.6	0.36
86457B	3.88	0.02	116	13.0	0.21	0.14	22.1	0.42
86457A	3.86	0.02	112	13.2	0.21	0.13	21.8	0.40
86450	0.00	0.02	358	10.4	2.19	1.01	17.5	4.35

*) above base of Tesero Horizon.

Table 17.
Abundances for Na, Mg, Al, K, Ca, Sc in Reppwand outcrop samples.

Sample No.	Cumulative thickness*) [m]	Thickness [m]	Ti [ppm]	V [ppm]	Cr [ppm]	Mn [ppm]	Fe [%]	Co [ppm]
86462	5.09	0.02	2970	76	54	258	2.57	11.3
86460	4.37	0.001	3900	61	59	212	2.17	13.1
86459C	4.23	0.02	510	14	14	180	0.65	1.1
86459B	4.21	0.02	<2500	13	9	188	0.59	0.9
86459A	4.19	0.02	710	11	10	184	0.68	5.4
86458	4.17	0.003	4670	121	92	98	16.29	39.5
86456D	4.08	0.02	720	10	8	166	0.55	0.8
86456C	4.05	0.02	750	11	8	168	0.49	0.8
86456B	4.03	0.02	560	9	7	166	0.48	0.7
86456A	4.01	0.02	780	11	8	161	0.62	1.1
86455	3.99	0.001	4680	84	62	161	5.54	17.7
86457E	3.96	0.02	<2600	5	3	165	0.53	0.4
86457D	3.93	0.02	<2000	3	3	158	0.49	0.2
86457C	3.91	0.02	<2000	3	3	154	0.47	0.3
86457B	3.88	0.02	<2100	6	3	152	0.53	0.3
86457A	3.86	0.02	<2500	< 3	3	150	0.49	0.5
86450	0.00	0.02	1590	34	32	139	1.17	5.2

*) above base of Tesero Horizon.

Table 18.
Abundances for Ti, V, Cr, Mn, Fe, Co in Reppwand outcrop samples.

3.1. Discussion of Figures

Our results have been formatted and illustrated in Text-Figs. 2 through 11, where we have selected a wide representation of elements for the Gartnerkofel-1 core samples. These figures have been prepared from the data presented in our tables. All ratios are expressed as weight to weight values. The Text-Figures 2–7 are plotted for the stratigraphic interval from about 75 to 330 m depth, similar to the interval plotted in Fig. 2 of W.T. HOLSER et al. (1989). Elemental abundances and ratios for the crucial interval form 175–135 m are plotted in Text-Figs. 8 to 11, with a stratigraphic column essentially the same as that of Fig. 3 in W.T. HOLSER et al. (1989). Carbon isotope data (M. MAGARITZ & W.T. HOLSER, 1989, this volume) are shown in several of the figures for orientation.

Descriptions for each of the figures are presented below:

Sample No.	Cumulative thickness*) [m]	Thickness [m]	As [ppm]	Rb [ppm]	Sb [ppm]	Cs [ppm]	Ba [ppm]	La [ppm]
86462	5.09	0.02	28.5	100	1.3	10.4	180	25.5
86460	4.37	0.001	22.2	71	·1.0	7.2	250	31.1
86459C	4.23	0.02	3.3	17	0.2	2.2	<160	8.1
86459B	4.21	0.02	2.5	14	0.1	1.9	<110	8.0
86459A	4.19	0.02	3.9	19	0.3	2.2	40	9.2
86458	4.17	0.003	218.	131	8.4	15.4	180	34.6
86456D	4.08	0.02	3.9	16	0.2	1.3	70	8.5
86456C	4.05	0.02	3.4	12	0.2	1.3	60	8.3
86456B	4.03	0.02	2.9	13	0.1	1.1	40	7.15
86456A	4.01	0.02	5.4	14	0.3	1.2	50	8.3
86455	3.99	0.001	176.	85	5.6	8.8	240	38.1
86457E	3.96	0.02	3.4	< 4	0.2	0.3	<100	3.5
86457D	3.93	0.02	1.8	< 5	0.0	0.3	<100	2.8
86457C	3.91	0.02	1.9	< 5	0.1	0.3	110	2.8
86457B	3.88	0.02	2.8	5	0.1	0.3	< 60	3.3
86457A	3.86	0.02	2.6	3	0.1	0.4	< 90	3.1
86450	0.00	0.02	14.8	39	0.6	4.4	60	17.1

*) above base of Tesero Horizon.

Table 19.
Abundances for As, Rb, Sb, Cs, Ba, La in Reppwand outcrop samples.

Sample No.	Cumulative thickness*) [m]	Thickness [m]	Ce [ppm]	Sm [ppm]	Eu [ppm]	Tb [ppm]	Dy [ppm]	Yb [ppm]
86462	5.09	0.02	46.7	4.4	0.8	0.4	3.3	1.7
86460	4.37	0.001	50.8	4.3	0.7	0.4	3.4	2.3
86459C	4.23	0.02	15.2	1.4	0.3	0.2	1.1	0.1
86459B	4.21	0.02	15.5	1.4	0.3	0.2	1.1	0.6
86459A	4.19	0.02	18.9	1.9	0.3	0.2	1.3	0.6
86458	4.17	0.003	67.9	3.8	0.8	0.6	3.7	2.8
86456D	4.08	0.02	15.8	1.7	0.3	0.2	1.1	0.8
86456C	4.05	0.02	13.7	1.5	0.3	0.2	1.5	0.7
86456B	4.03	0.02	12.0	1.2	0.3	0.2	1.2	0.6
86456A	4.01	0.02	16.3	1.1	0.3	0.2	1.1	0.8
86455	3.99	0.001	56.1	4.5	0.8	0.5	3.6	2.8
86457E	3.96	0.02	5.4	0.6	0.1	0.1	<4.1	0.2
86457D	3.93	0.02	5.5	0.5	0.1	<0.2	<2.8	0.2
86457C	3.91	0.02	4.2	<2.8	0.1	<2.8	0.2	
86457B	3.88	0.02	5.4	0.5	0.1	0.1	<2.7	0.28
86457A	3.86	0.02	5.1	0.5	0.1	0.1	< 3.9	0.2
86450	0.00	0.02	27.5	2.9	0.6	0.4	1.4	

*) above base of Tesero Horizon.

Table 20.
Abundances of Ce, Sm, Eu, Tb, Dy, Yb in Reppwand outcrop samples.

Figure 2

Abundances are plotted for the common elements, Al, Mg, Ca and Fe. The Al concentration reflects the relative clay content of the samples. The large Mg component reflects the pervasive dolomitization of the whole section (K. BOECKELMANN & M. MAGARITZ, this volume). The iron plot points out the strong Fe pyrite enrichment at 185 m (sample 117), and an intermediate enrichment at 225 m (samples 196).

Figure 3

Iridium abundances are compared with $\delta^{13}C$ taken from W.T. HOLSER et al. (1989). The Ir is plotted by itself, taken as a ratio to Al (Al is representative of the clay fraction), and on a carbonate-free basis (to avoid false anomalies caused by carbonate dissolution). In the carbonate-free basis, Mg and Ca are assumed to be present entirely in the carbonate form. The equation for this correction to Ir is thus:

Sample No.	Cumulative thickness*) [m]	Thickness [m]	Lu [ppm]	Hf [ppm]	Ta [ppm]	Ir [ppt]	Th [ppm]	U [ppm]
86462	5.09	0.02	0.26	2.9	0.9	40	7.6	9.4
86460	4.37	0.001	0.33	5.6	1.2	34	9.2	9.9
86459C	4.23	0.02	0.08	0.6	0.2	5	1.8	2.8
86459B	4.21	0.02	0.07	0.6	0.2	4	1.5	2.4
86459A	4.19	0.02	0.09	0.7	0.1	5	2.1	2.5
86458	4.17	0.003	0.43	7.5	1.3	220	14.5	18.6
86456D	4.08	0.02	0.10	1.4	0.2	4	1.8	2.9
86456C	4.05	0.02	0.10	1.4	0.2	< 2	1.7	3.0
86456B	4.03	0.02	0.09	0.9	<0.2	< 2	1.3	2.6
86456A	4.01	0.02	0.10	1.6	<0.2	5	1.8	2.8
86455	3.99	0.001	0.37	7.4	1.2	100	11.9	16.0
86457E	3.96	0.02	0.03	0.1	<0.2	3	0.4	1.1
86457D	3.93	0.02	<0.04	0.1	<0.2	< 2	0.3	1.0
86457C	3.91	0.02	0.04	<0.2	<0.2	< 2	0.3	1.0
86457B	3.88	0.02	0.1	0.1	<0.2	3	0.4	1.2
86457A	3.86	0.02	0.03	0.1	<0.2	3	0.4	1.2
86450	0.00	0.02	0.19	1.9	0.5	17	4.3	4.4

*) above base of Tesero Horizon.

Table 21.
Abundances of Lu, Hf, Ta, Ir, Th, U in Reppwand outcrop samples.

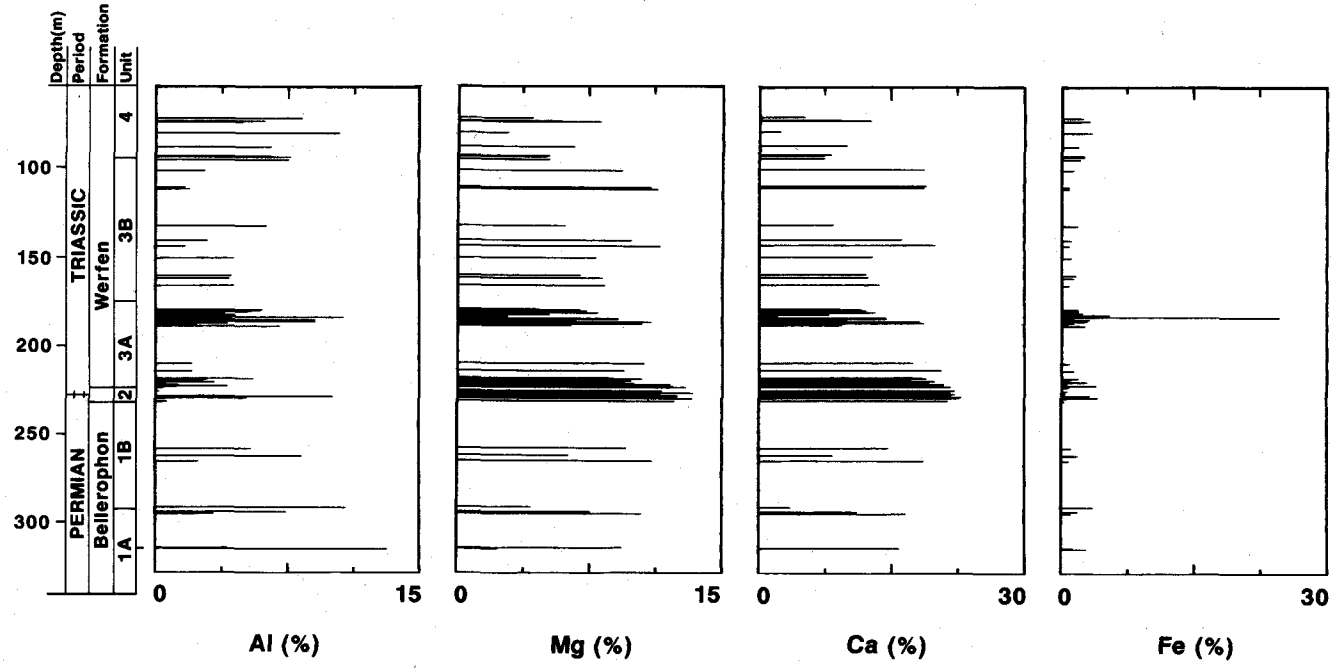

Text-Fig. 2.

Ir/[1−(0.025 × wt % Ca + 0.0347 × wt % Mg)].

When a sample is essentially pure carbonate, this calculation can lead to very large errors because a number very close to unity is subtracted from unity; uncertainties in measurement can easily lead to a negative number in the denominator. From these Ir data, in particular the Ir/Al plot, we conclude that the excess Ir in the two peak regions is the result of some process(es) different from those occurring in the bulk of the section. Apparently the process(es) also involve a deficiency of ^{13}C in carbonates over pre-boundary levels.

Figure 4

Iridium is plotted as ratios to Cr, Fe, Co and As. The primary reason for the Ir/Fe plot is to show that the Ir in samples 117 is not enriched as much over local background as is Fe (as pyrite). However, Ir/Fe is considerably above local background ($\approx 1.2 \times 10^{-9}$) just below sample 117 and in the stratigraphic interval of Unit 2 (P-Tr boundary interval).

The Ir/As plot indicates, that except for an occasional deviation, Ir correlates quite well with As.

The Ir/Cr and Ir/Co ratios can provide some information about possible extraterrestrial contributions to

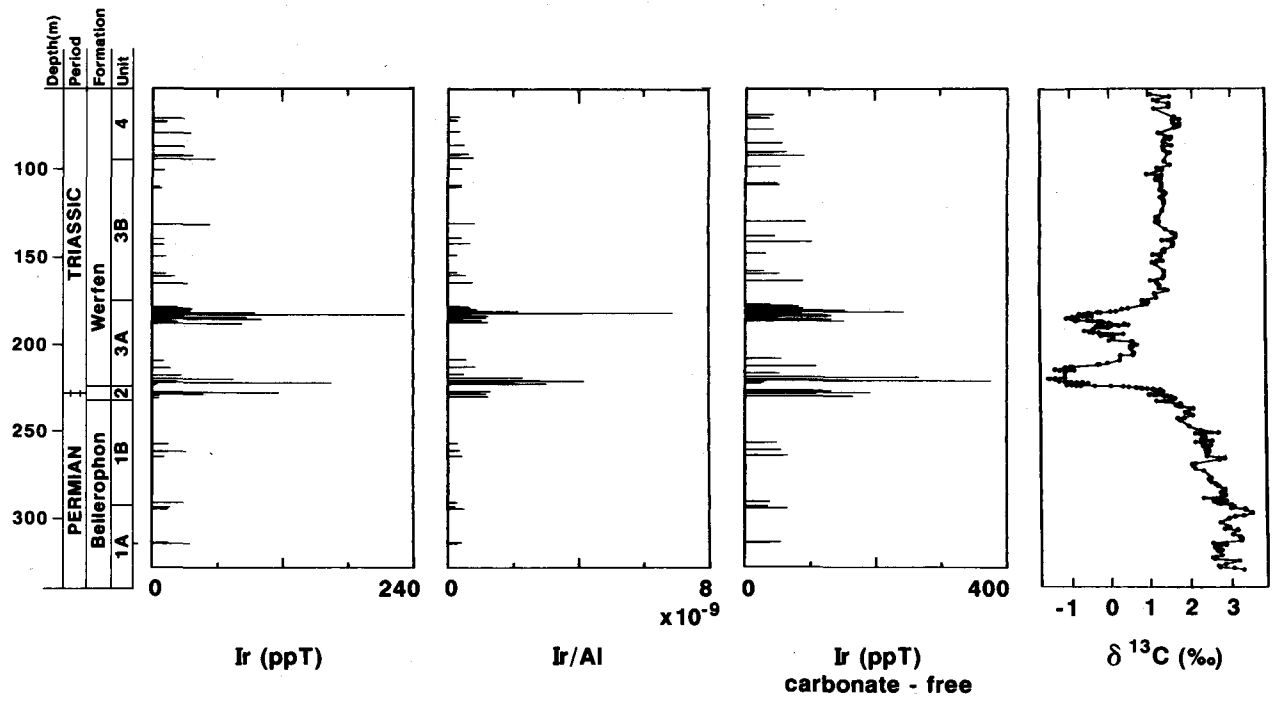

Text-Fig. 3.

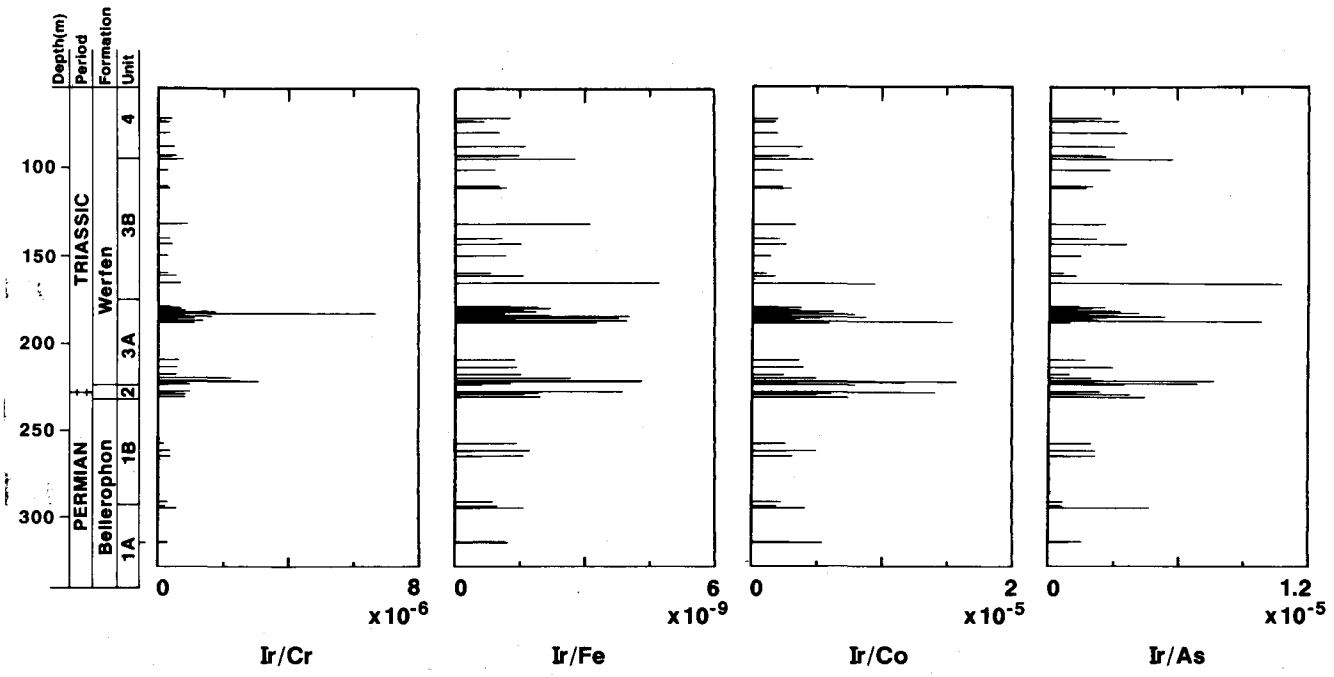

Text-Fig. 4.

the two Ir maxima at 185.57 m (sample 117) and 224.52 m (sample 196). Solar system or C1 chondrite ratios are: Ir/Cr ≈ 4.9×10^{-5} and Ir/Co ≈ 2.9×10^{-4} (P. HENDERSON, 1982). The background Ir/Cr level from the plot is about 4×10^{-7}, typical of terrestrial rocks and especially chromites, but about two orders of magnitude smaller than chondritic. At the samples 117 peak the ratio increases about twenty-fold to 7×10^{-6}. This is still an order of magnitude smaller than chondritic. In the boundary interval (samples 196) the Ir to Cr enhancement is about half that at the upper peak.

The Ir/Co ratio in sample 117 is identical to local background. In the boundary interval (samples 196 and 203), Ir/Co ≈ 1.4×10^{-5}, twenty-fold lower than chondritic.

Figure 5

Abundance patterns for V, Cr, Co and U are expressed as ratios to Al. The ratios provide a better indication (as was the case with Ir) than the pure elements of anomalous trends because the section contains a mixture of carbonates and shales or marls and these elements tend to associate with the clay or detrital fraction. Cr and U display normal behaviour in the pyrite samples (117), but show some enrichment just prior to and in the P-Tr boundary interval. Co and V show two-

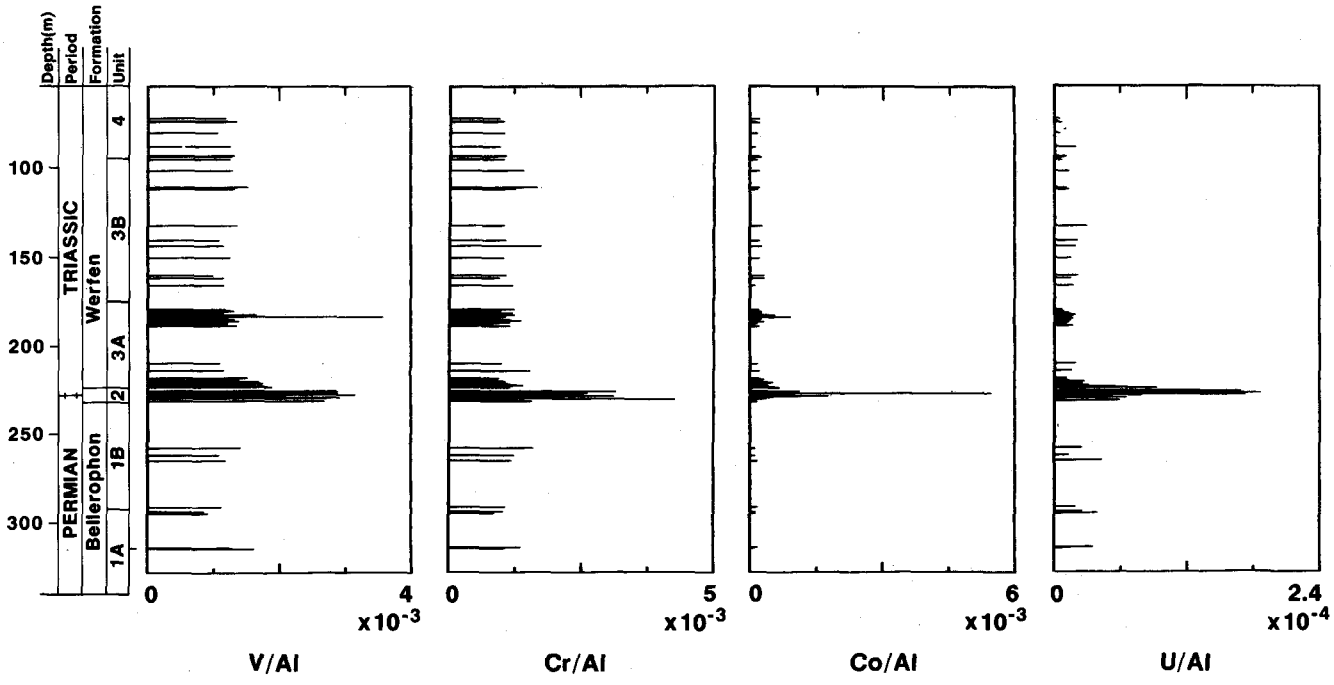

Text-Fig. 5.

to three-fold enrichment in the pyrite and are also enhanced in the lower portion of the P-Tr interval.

Figure 6

The first plot of the rare-earth pattern shows La expressed as a ratio to Al. La was selected as the representative rare earth because it is determined with good precision by the INAA method. We note that La (rare earth) concentrations are anomalously high just below and at the P-Tr-boundary interval. Also, La/Al is about 1.5 to 2 times greater above the boundary than it is below.

Cerium, which exhibits both III-and IV-valence states, has been used as an indicator of redox conditions during deposition. However, mechanisms for removal from seawater and diagenetic processes as well as the incorporation in detrital material may make interpretation of Ce data difficult and ambiguous. We observe a slight monotonic decrease of the Ce/La ratio from the bottom to the top of the core and, more importantly, a noticeable decrease just before and at the P-Tr boundary interval. We chose to plot the inverse (La/Ce) to obtain a peak rather than a valley in the anomalous zone.

The last two plots, Yb/La and Lu/La, provide information about heavy-to-light rare-earth ratios which are seen to be slightly enhanced in the rare-earth anomaly zone. Relative to average crustal rocks, the ratio of

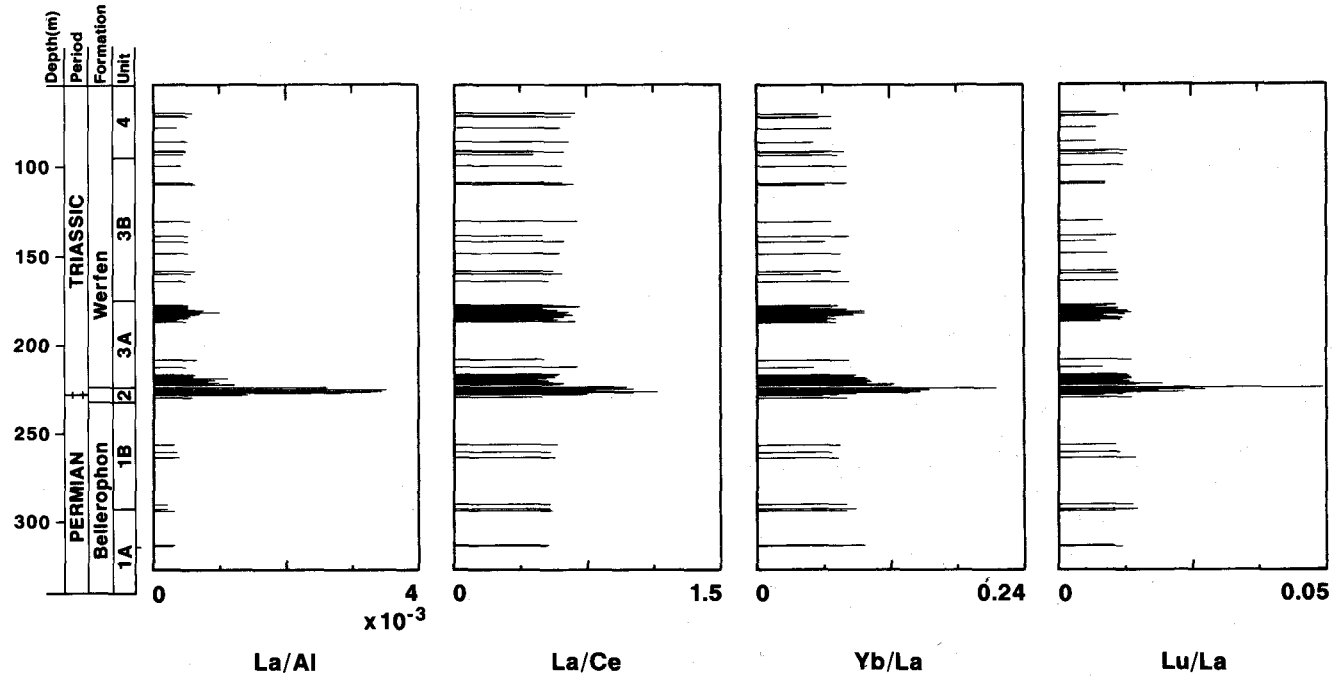

Text-Fig. 6.

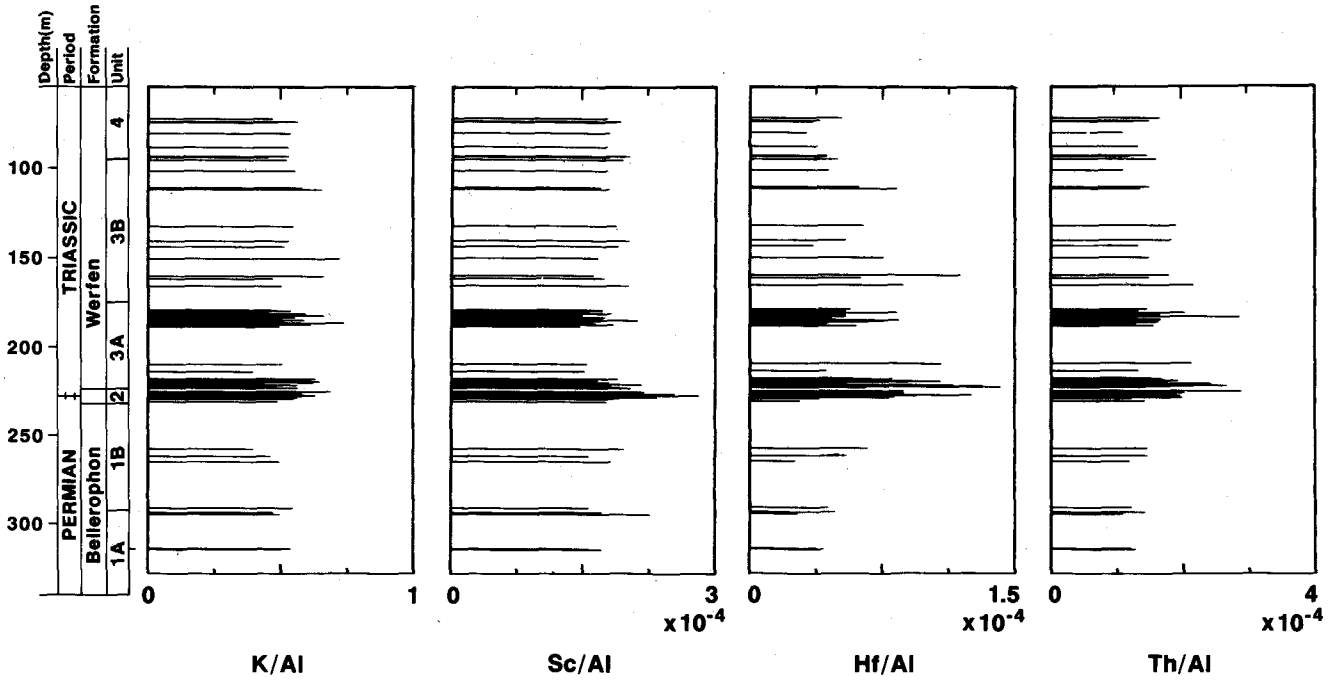

Text-Fig. 7.

heavy to light is greater in meteorites (E. ANDERS & M. EBIHARA, 1982), ultramafic rocks (E. JAGOUTZ et al., 1979) and in ocean water (P. HENDERSON, 1982).

The facts that rare-earth concentrations increase in the lower anomaly zone at and just below the Tesero Horizon, Ce/La decreases and Yb/La and Lu/La increase lead us to suspect that these ratios were largely the result of precipitation mechamisms from ocean water in this stratigraphic interval.

Figure 7

Patterns for some selected lithophiles are also expressed as ratios to Al. Generally these elements act similarly to Al unless perturbation occurs, e. g. erosion of ultramafic source rocks would tend to increase Sc/Al and to decrease Hf/Al and Th/Al, and altered ash (bentonites) from some silicic volcanoes might show the opposite. In this section K and Sc show a very strong correlation with Al and the ratios are essentially

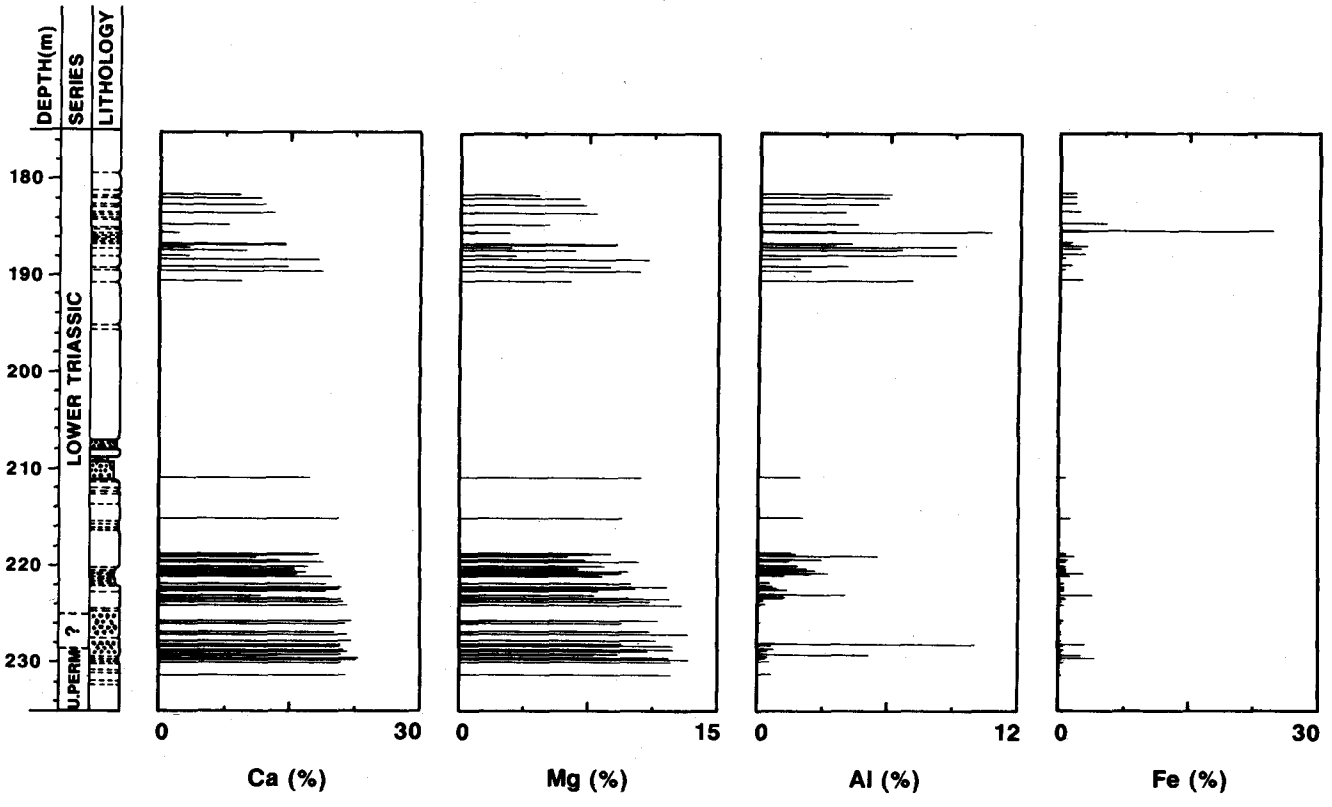

Text-Fig. 8.

flat throughout. If an imaginary line were drawn through the average values of Hf/Al and Th/Al, an increase would be observed just before the P-Tr boundary, followed by a subtle monotonic decrease. It is not obvious what this indicates, perhaps sedimentation derived from source rocks of more mafic to ultramafic composition in the upper portion of the core (A. FENNINGER, this volume).

Figure 8

Abundance patterns are shown for some common elements in the stratigraphic interval from 175 to 235 m.

Figure 9

Abundances for Ir, Cr, Fe, and Co are expressed as a ratio to Al. In and just below the Tesero Horizon, Cr/Al, Fe/Al, and Co/Al show maxima for the section. Although Ir was not analyzed in all samples, Ir/Al does not appear to exceed local background in this unit (2), but reaches a peak or maximum just above the Tesero Horizon and after the rare-earth anomalies.

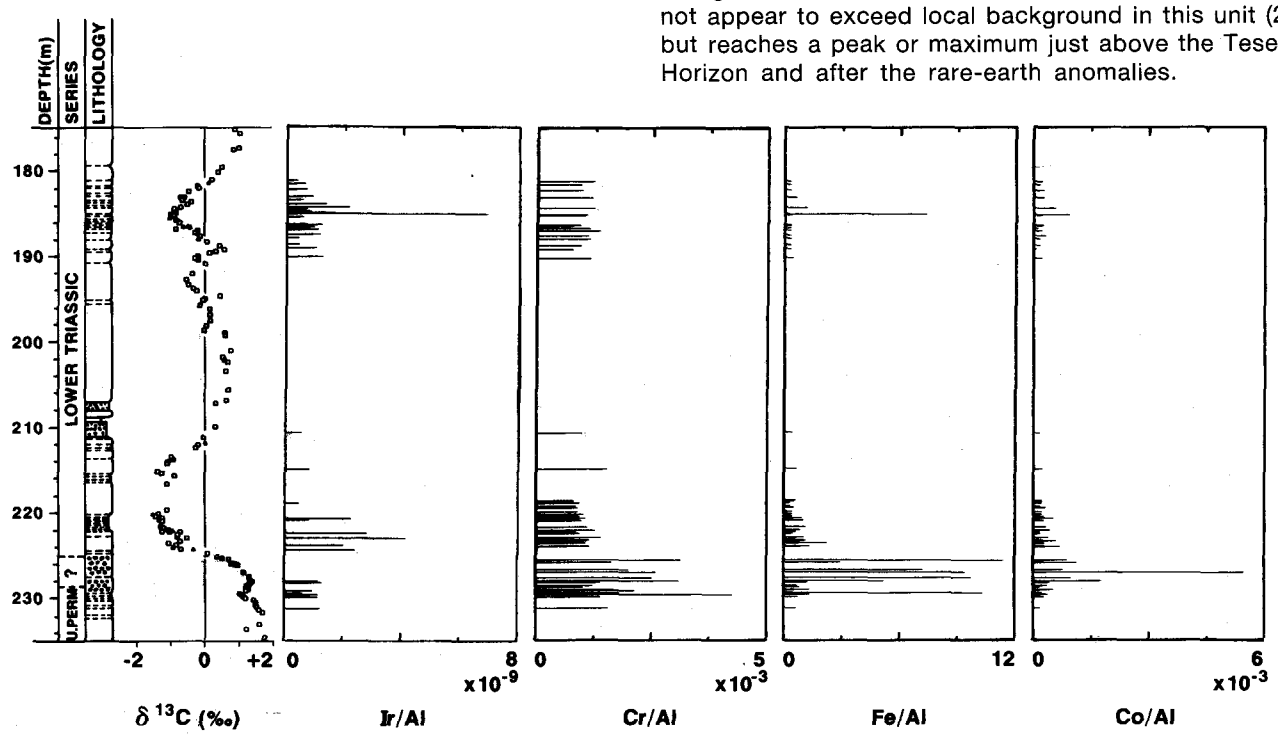

Text-Fig. 9.

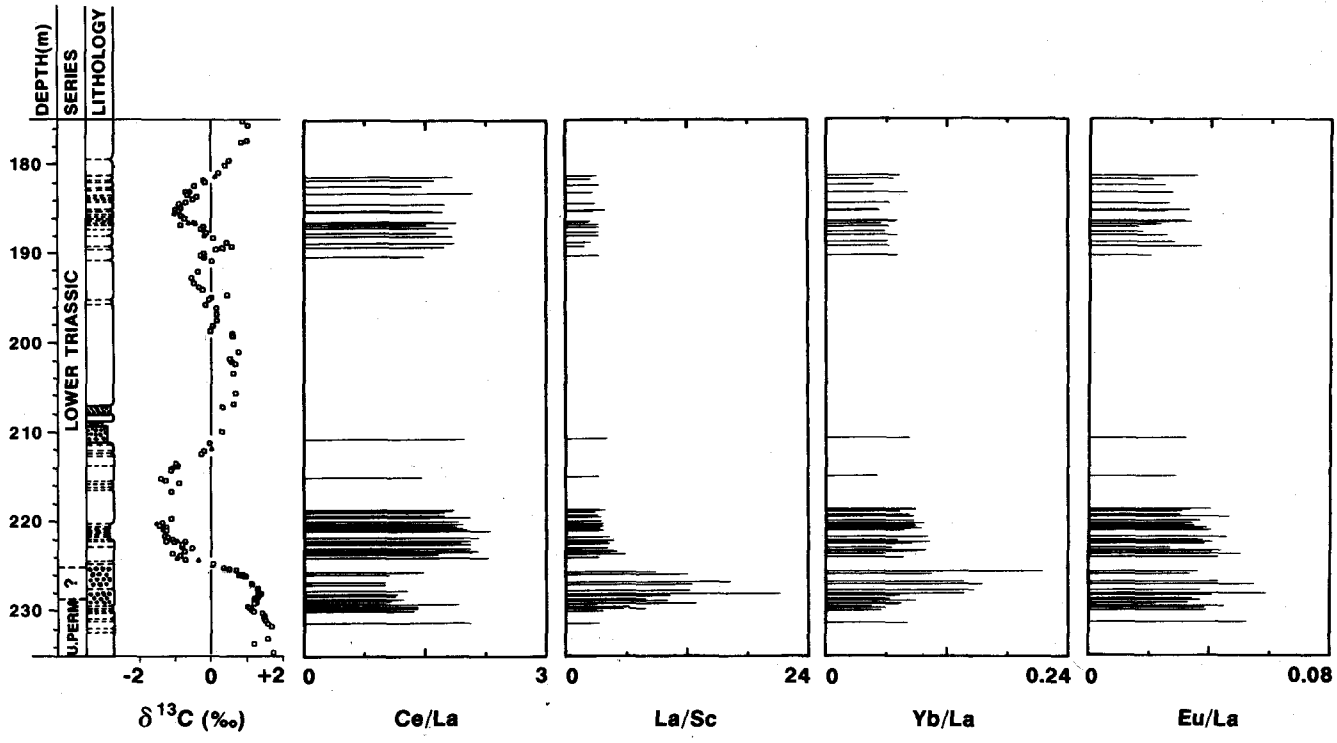

Text-Fig. 10.

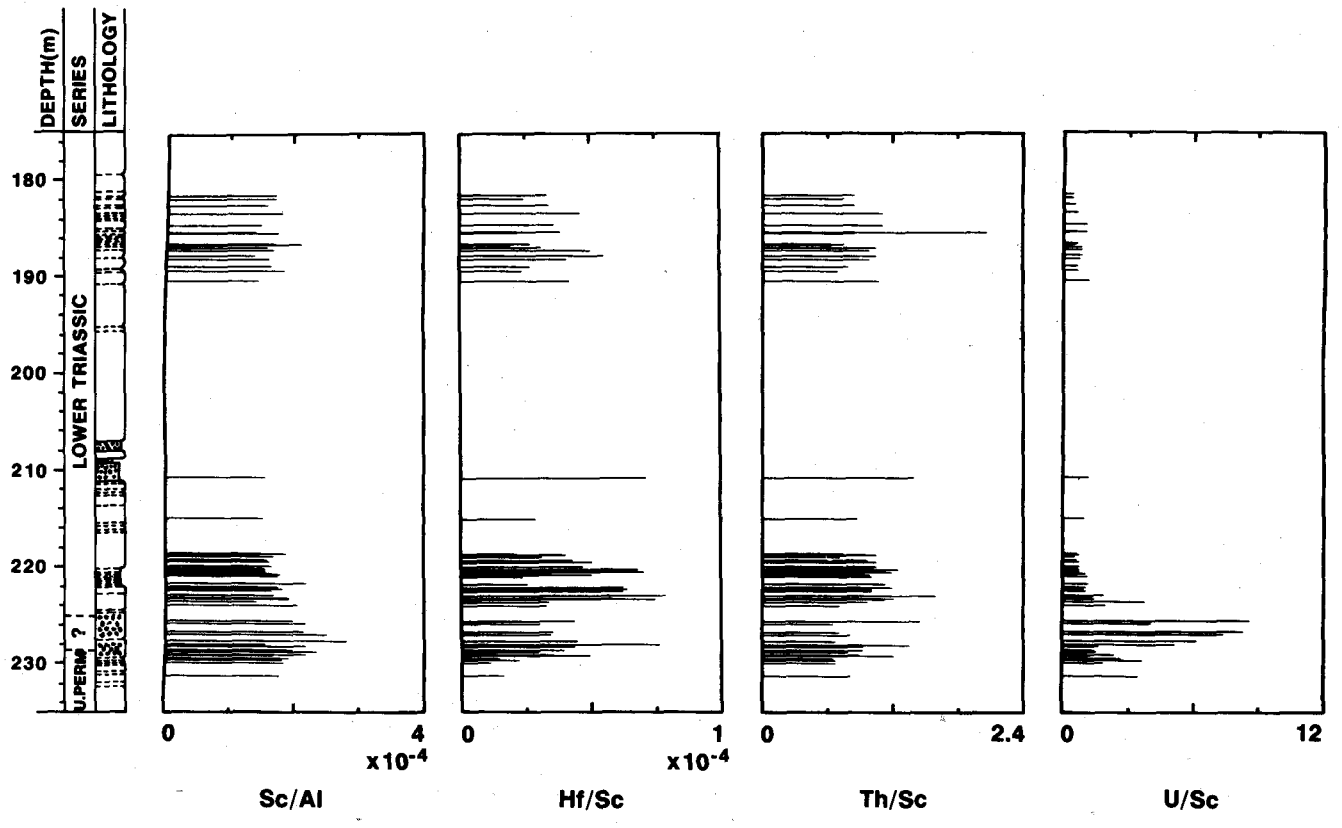

Text-Fig. 11.

Figure 10

These rare-earth profiles are similar to those in Fig. 6. We plot La as a ratio to Sc rather than Al because the correlation of Sc with Al is high and Sc is determined with greater precision than is Al. The points are spread out more than in Fig. 5, so the conventional Ce/La ratio was plotted rather than the inverse. A middle-weight rare earth (Eu) was plotted as a ratio to La in the place of the Lu/Al profile. There is no obvious peak in the Eu/La diagram as there is with La/Sc, Yb/la and Ce/La (valley).

Figure 11

Profiles for some lithophile elements are expressed as a ratio to Al or Sc. The Sc/Al profile demonstrates the high correlation of Sc with Al. In this stratigraphic interval, values of Hf/Sc and Th/Sc show very little deviation from the averages. On the contrary, U/Sc shows a broad maximum in and below the Tesero Horizon (Unit 2); the significance is not obvious.

4. Conclusions

Elemental abundance and ratio profiles across the Gartnerkofel-1 core indicate two concentration maxima for Ir. Both maxima roughly coincide with shifts to the lighter isotope of carbon in the carbonates. The upper maximum at 185.57 m (sample 117) is sharp and associated with a pyrite bed. Ir and chalcophiles like As and Sb are enriched in this bed by an order of magnitude over local backgrounds. There are no obvious indications that the Ir enrichment is associated with a large-body impact. Iridium appears to be associated with the pyrite formation, which we have observed in several other black shale sequences.

The lower Ir peak, at 224.5 m (sample 196), is somewhat of an enigma because it occurs above the $\delta^{13}C$ "edge", where also rare earth and other elemental ratio profiles change. On the basis of our present elemental abundance evidence it is impossible to completely preclude some contribution to the Ir excess from an extraterrestrial source. However, Ir peaks in the P-Tr boundary interval are about two orders of magnitude weaker than the Ir-anomaly at well-preserved K-T boundary sections. Furthermore, the Ir/Cr and Ir/Co weight ratios are at least an order of magnitude smaller than chondritic ratios, but similar to those in terrestrial rocks. And also, on the basis of the lack of physical evidence (neither microspherules nor shocked-mineral grains were found in this horizon), the lower Ir peak appears to be associated with reducing conditions similar to the situation in sample 117.

Broad concentration maxima of some elements, expressed as a ratio to Al or Sc, occur in and just below the Tesero Horizon. It should be noted that the element concentrations themselves are quite low in some of the samples from this interval because of the large carbonate and small detrital clay contributions. Enhanced ratios include those for rare earths, V, Fe, Co, As, Sb, and U; the Ir/Al maximum occurs above where the other ratios reach their peaks and Ir itself is enriched in the shaly horizon above the Tesero. In the Tesero the enhancement mechanism is not obvious, but one possible process can be inferred from the INAA abundance data and the results for S, $\delta^{13}C$ and $\delta^{18}O$ (HOLSER, this volume; KLEIN, this voume; MAGARITZ & HOLSER, this volume). The S data suggest anoxic conditions just above the Tesero Horizon and in the pyrite-rich zone at

≈ 185.5 m. Depositional conditions in the Tesero Horizon appear to have been oxic on the bases of oolite presence and low S content. Therefore, the valley in Ce/La (Fig. 10) is probably not redox related. Rather, we suggest that the dip in Ce/La enhancements of RE/Al, RE/Sc, Yb/La and Lu/La were the result of increased scavenging of these REs from ocean water, under oxygenated conditions. A bothersome feature of this scenario is the relative flatness of the Eu/La profile (Fig. 10). A valley similar to that in the Ce/La profile might be expected because Eu is depleted in ocean water (Eu/La = 0.0035) relative to crustal rocks (Eu/La = 0.040) (P. HENDERSON, 1982).

Acknowledgements

We thank the members of the Los Alamos Research Reactor Group for the neutron irradiations, and especially S.R. GARCIA and J.S. NEWLIN for providing elemental abundances with the automated INAA system. This work was supported by the National Aeronautics and Space Administration (Planetary Materials and Geochemistry Program) and the U. S. Department of Energy (Basic Energy Sciences).

References

ANDERS, E. & EBIHARA, M.: Solar System Abundances of the Elements. – Geochim. Cosmochim. Acta **46**, 2363–2380, New York 1982.

CLARK, D.L., WANG, C.-Y., ORTH, C.J. & GILMORE, J.S.: Conodont Survival and Low Iridium Abundances across the Permian-Triassic Boundary in South China. – Science, **233**, 984–986, Washington 1986.

HENDERSON, P.: Inorganic Geochemistry. – 353 pp., New York (Pergamon Press) 1982.

HOLSER, W.T., SCHÖNLAUB, H.P., ATTREP, M., Jr., BOECKELMANN, K., KLEIN, P., MAGARITZ, M., ORTH, C.J., FENNINGER, A., JENNY, C., KRALICH, M., MAURITSCH, H., PAK, E., SCHRAMM, J.M. STATTIGER, K. & SCHMOLLER, R.: A Unique Geochemical Record at the Permian-Triassic Boundary. – Nature, **337**, 39–44, London 1989.

JAGOUTZ, E., PALME, H., BADDENHAUSEN, H., BLUM, K., CENDALES, M., DREIBUS, G., SPETTEL, B., LORENZ, V. & WANKE, H.: The Abundances of Major, Minor and Trace Elements in the Earth's Mantle as Derived from Primitive Ultramafic Nodules. – Proceedings 10th Lunar and Planetary Science Conference, 2031–2050, Houston 1979.

MINOR, M.M., HENSLEY, W.K., DENTON, M.M. & GARCIA, S.R.: An Automated Neutron Activation Analysis System. – Radioanalyt. Chem., **70**, 459–471, Budapest 1981.

ORTH, C.J., ATTREP, M., Jr. & QUINTANA, L.R.: Iridium Abundance Measurements across Bio-Event Horizons in the Fossil Record. – Abstr. Conference on Global Catastrophies in Earth History, Snowbird, Utah, October 20.–30., 139–140, 1988. Also to be published in the Conference Proceedings.

RAUP, D.M. & SEPKOSKI, J.J., Jr.: Periodicity of Extinctions in the Geologic Past. – Proc. Nat. Acad. Sci., **81**, 801–805, Washington 1984.

RAUP, D.M. & SEPKOSKI, J.J., Jr.: Periodic Extinctions of Families and Genera. – Science, **231**, 833–836, Washington 1986.

SEPKOSKI, J.J., Jr.: Mass Extinctions in the Phanerozoic Oceans: A Review. – In: SILVER, L.T. & SCHULTZ, P.H. (eds.): Geol. Soc. Amer. Special Paper 190, Geological Implications of Impacts of Large Asteroids and Comets on the Earth, 283–289, Boulder 1982.

SUN, Y., CHAI, Z., MA, S., MAO, X, XU, D., ZHANG, Q., YANG, Z., SHENG, J., CHEN, C., RUI, L., LIANG, X., ZHAO, J. & HE, J.: Discovery of Anomalies of Platinum-Group Elements at the Permian-Triassic Boundary in Changxing, Zhejiang, China and their Significance. – Abstr. 27th Intern. Geol. Congr., Rare Events in Geology, **8**, 309, Moscow 1985.

XU, D., MA, S., CHAI, Z., MAO, X., SUN, Y., ZHANG, Q & YANG, Z.: Abundance Variation of Iridium and Trace elements at the Permian/Triassic Boundary at Shangsi in China. – Nature, **314**, 154–156, London 1985.